© 2017. Published by The Company of Biologists Ltd | Development (2017) 144, 2730-2736 doi:10.1242/dev.143370

Soluble APP functions as a vascular niche signal that controls adult neural stem cell number

Yuya Sato[1], Yutaka Uchida[1], Jingqiong Hu[1,2], Tracy L. Young-Pearse[3], Takako Niikura[4] and Yoh-suke Mukouyama[1,*]

ABSTRACT

The molecular mechanism by which NSC number is controlled in the neurogenic regions of the adult brain is not fully understood but it has been shown that vascular niche signals regulate neural stem cell (NSC) quiescence and growth. Here, we have uncovered a role for soluble amyloid precursor protein (sAPP) as a vascular niche signal in the subventricular zone (SVZ) of the lateral ventricle of the adult mouse brain. sAPP suppresses NSC growth in culture. Further *in vivo* studies on the role of APP in regulating NSC number in the SVZ clearly demonstrate that endothelial deletion of *App* causes a significant increase in the number of BrdU label-retaining NSCs in the SVZ, whereas NSC/astrocyte deletion of *App* has no detectable effect on the NSC number. Taken together, these results suggest that endothelial APP functions as a vascular niche signal that negatively regulates NSC growth to control the NSC number in the SVZ.

KEY WORDS: APP, Neural stem cell, Subventricular zone, Vascular niche

INTRODUCTION

The vascular niche is now firmly established as a microenvironment that sustains tissue progenitors in close proximity to blood vessels (Rafii et al., 2016). In the neurogenic regions of the adult brain – the subventricular zone (SVZ) of the lateral ventricle and the subgranular zone (SGZ) of the dentate gyrus of the hippocampus (Kriegstein and Alvarez-Buylla, 2009; Ming and Song, 2005; Zhao et al., 2008) – neural stem cells (NSCs) are located in close proximity to specialized capillary endothelial cells (ECs) (Palmer et al., 2000; Shen et al., 2008; Tavazoie et al., 2008). Emerging evidence suggests that these ECs provide signals that direct NSC quiescence and growth (Rafii et al., 2016). In the SVZ, endothelial neurotrophin 3 (NT-3) and ephrin B2 control NSC quiescence as a soluble paracrine and cell-cell contact-dependent signal, respectively (Delgado et al., 2014; Ottone et al., 2014), and endothelial brain-derived neurotrophic factor (BDNF) (Leventhal et al., 1999), pigment epithelium-derived factor (PEDF; also known as Serpinf1) (Ramirez-Castillejo et al., 2006), betacellulin (Gomez-Gaviro et al., 2012) and placental growth factor 2 (PlGF-2) (Crouch et al., 2015) stimulate NSC growth. These studies raise an intriguing question about how multiple vascular signals coordinate NSC quiescence and growth.

Amyloid precursor protein (APP) is widely expressed throughout the adult mouse brain, including in neurogenic regions such as the SVZ (Caille et al., 2004) and SGZ (Guo et al., 2012; Wang et al., 2014), and affects embryonic and adult neurogenesis in mice (Baratchi et al., 2012; Caille et al., 2004; Ma et al., 2008; Wang et al., 2014, 2016). The secreted form of APP (soluble APP, sAPP) has been reported to enhance proliferation of SVZ-NSCs (Baratchi et al., 2012; Caille et al., 2004; Ohsawa et al., 1999) and SGZ-NSCs (Baratchi et al., 2012). Interestingly, infusion of sAPP increased the proliferation of epidermal growth factor (EGF)-responsive neurosphere-forming SVZ-NSCs *in vivo* (Caille et al., 2004), whereas *App* deficiency enhanced the proliferation of neural progenitors in the SGZ (Wang et al., 2014, 2016). Despite the significant roles of APP in adult neurogenesis, the potential involvement of APP as a vascular niche signal in maintaining SVZ-NSCs has not been studied.

In this study, we attempted to identify EC-derived soluble signals that control NSC number in the SVZ. We found that brain microvascular EC line (bEND3)-derived conditioned medium (CM) increased the number of SVZ-derived neurospheres and decreased the size of individual neurospheres in culture. One of the 29 proteins we identified from the bEND3-CM, sAPP, was shown to enhance neurosphere-forming potential but suppress NSC growth in culture. Furthermore, our extensive studies in conventional and cell type-specific mutant mice clearly demonstrate that endothelial APP negatively regulates NSC number in the SVZ.

RESULTS AND DISCUSSION

Brain EC-derived soluble factors enhance neurosphere-forming potential but suppress NSC growth in culture

To improve our understanding of the nature of vascular niche signals for NSC maintenance, we used an established neurosphere culture (passaged neurospheres) from adult mouse SVZ cells (Fig. 1A). Passaged neurospheres were cultured with a medium conditioned by bEND3 cells, which have been reported to support NSCs (Ottone et al., 2014; Shen et al., 2004). We found that the bEND3-CM increased the number of SVZ-derived neurospheres and decreased the size of individual neurospheres (Fig. 1B-E). After cells had been treated with bEND3-CM, secondary neurospheres formed in normal growth medium at a significantly higher number but with a smaller size (Fig. 1F,G), suggesting that the bEND3-CM enhances neurosphere-forming potential but suppresses NSC growth in culture. The bEND3-CM treatment did not affect multipotency of SVZ-NSCs, as differentiation of neurospheres into neurons, astrocytes and oligodendrocytes was observed (Fig. 1H-M). No significant pro-differentiative effects of bEND3-

[1]Laboratory of Stem Cell and Neuro-Vascular Biology, Genetics and Developmental Biology Center, National Heart, Lung, and Blood Institute, National Institutes of Health, Building 10/6C103, 10 Center Drive, Bethesda, MD 20892, USA. [2]Stem Cell Center, Wuhan Union Hospital, Tongji Medical College, Huazhong University of Science and Technology, Wuhan, Hubei 430022, China. [3]Ann Romney Center for Neurologic Diseases, Brigham and Women's Hospital and Harvard Medical School, 77 Avenue Louis Pasteur, Boston, MA 02115, USA. [4]Department of Information and Communication Sciences, Faculty of Science and Technology, Sophia University, 7-1 Kioi-cho, Chiyoda-ku, Tokyo 102-8554, Japan.

*Author for correspondence (mukoyamay@mail.nih.gov)

J.H., 0000-0002-0284-7235; Y.M., 0000-0002-9084-4922

Received 5 August 2016; Accepted 29 June 2017

Development (2017) 144, 2730-2736 doi:10.1242/dev.143370

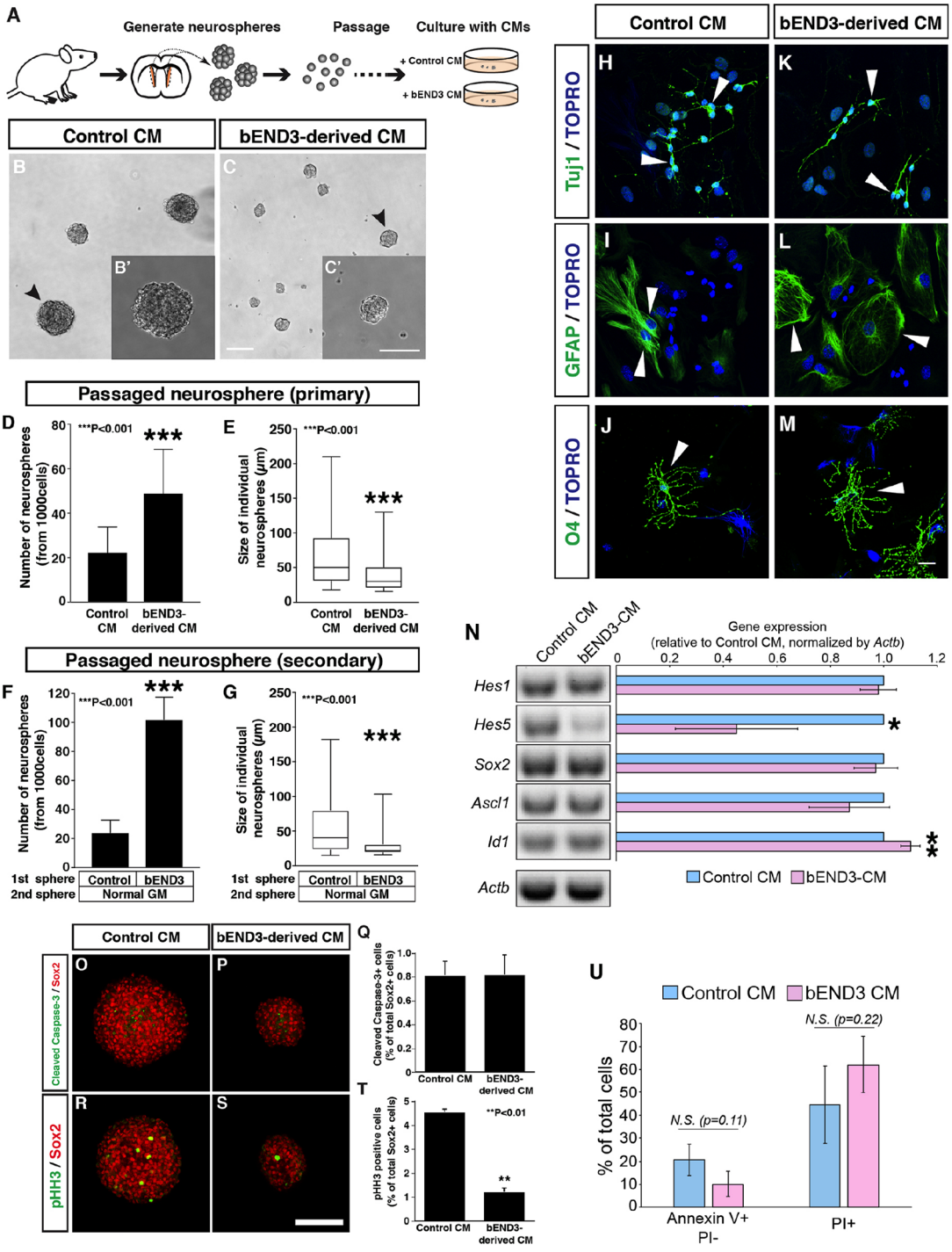

Fig. 1. Brain EC-derived soluble factors influence SVZ-NSC behaviors in culture. (A) Schematic of the experimental design. (B,C) Images of typical passaged neurospheres in the medium containing CM from fresh Opti-MEM (control CM) or bEND3 culture (bEND3-derived CM). Individual neurospheres (arrowheads) are magnified in the insets (B′,C′). (D,E) Quantification of primary neurosphere number (D; *n*=16 wells of 96-well plates from four independent experiments) and size (E; *n*=172 and 348 individual neurospheres in the control and bEND3-CM, respectively, from three independent experiments). (F,G) Quantification of secondary neurosphere number (F; *n*=16 from four independent experiments) and size (G; *n*=256 and 646 in control and bEND3-CM, respectively, from four independent experiments). Individual passaged neurospheres from the culture containing bEND3-CM and control CM were dissociated by trituration, and then re-plated at clonal density in the normal neurosphere growth medium (GM) without any CM. (H-M) Representative images showing the differentiation of passaged neurospheres into Tuj1 (Tubb3)$^{+}$ neurons (H,K, green), GFAP^{+} astrocytes (I,L, green) and O4^{+} oligodendrocytes (J,M, green). Nuclei were stained with TO-PRO-3 (blue). (N) RT-PCR analysis of *Hes1*/*5*, *Sox2*, *Ascl1* and *Id1* expression in passaged neurospheres (left panel). Right panel shows quantification of gene expression relative to *Actb* from three independent experiments. (O,P) Whole-mount neurosphere staining with antibodies to a cell death marker, cleaved caspase-3 (green), together with an NSC marker, Sox2 (red). (Q) Quantification of cleaved caspase-3^{+} dying cells. (R,S) Whole-mount neurosphere staining with antibodies to a proliferation marker, phospho-histone H3 (pHH3, green), and Sox2 (red). (T) Quantification of pHH3^{+} NSCs. (U) Cell viability was assessed by the apoptosis marker Annexin V-Alexa488 and the dead cell marker propidium iodide (PI) after plating for 24 h in the presence of control CM or bEND3-CM. Bars represent mean±s.d. **P*<0.05; ***P*<0.01; ****P*<0.001 (Student's *t*-test). Scale bars: 100 µm (B-C′,O-S); 20 µm (H-M).

Development (2017) 144, 2730-2736 doi:10.1242/dev.143370

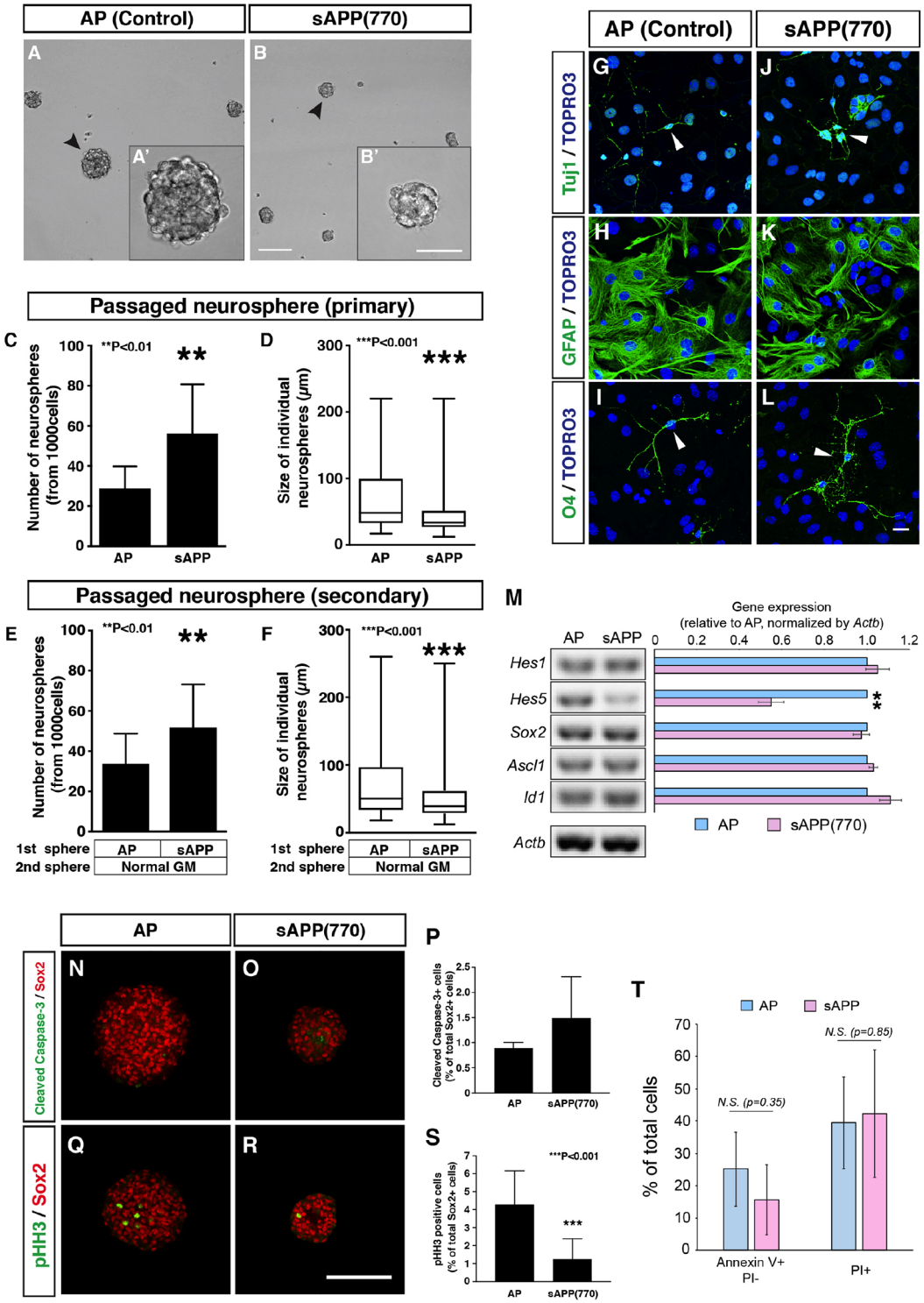

Fig. 2. Soluble APP serves as an EC-derived signal to influence SVZ-NSC behaviors in culture. (A,B) Images of typical passaged neurospheres grown in the presence of control alkaline phosphatase (AP) or sAPP(770). Individual neurospheres (arrowheads) are magnified in the insets (A′,B′). (C,D) Quantification of primary neurosphere number (C; *n*=12 wells of 96-well plates from three independent experiments) and size [D; *n*=166 and 312 individual neurospheres in control AP and sAPP(770), respectively, from three independent experiments]. (E,F) Quantification of secondary neurosphere number (E; *n*=16 from four independent experiments) and size [F; *n*=209 and 294 in control AP and sAPP(770), respectively, from four independent experiments]. (G-L) Representative images showing the differentiation of passaged neurospheres into Tuj1$^+$ neurons (G,J, green), GFAP$^+$ astrocytes (H,K, green) and O4$^+$ oligodendrocytes (I,L, green). Nuclei were stained with TO-PRO-3 (blue). (M) RT-PCR analysis of *Hes1*/*5*, *Sox2*, *Ascl1* and *Id1* expression in passaged neurospheres (left panel). Right panel shows quantification of gene expression relative to *Actb* from three independent experiments. (N,O) Whole-mount neurosphere staining with antibodies to cleaved caspase-3 (green) and Sox2 (red). (P) Quantification of cleaved caspase-3$^+$ dying cells. (Q,R) Whole-mount neurosphere staining with antibodies to pHH3 (green) and Sox2 (red). (S) Quantification of pHH3$^+$ NSCs. (T) Cell viability was assessed by Annexin V-Alexa488 and PI after plating for 24 h in the presence of control AP or sAPP(770). Bars represent mean±s.d. ***P*<0.01; ****P*<0.001 (Student's *t*-test). Scale bars: 100 µm (A,B); 50 µm (A′,B′); 20 µm (G-L); 100 µm (N-R).

Development (2017) 144, 2730-2736 doi:10.1242/dev.143370

CM on NSCs were observed in culture (Fig. S1). We further examined the expression of key transcription factors such as *Hes1/5*, *Sox2*, *Ascl1* (also known as *Mash1*) and *Id1-4*, which are characteristic of NSCs (Jung et al., 2010; Nam and Benezra, 2009; Ramirez-Castillejo et al., 2006). The bEND3-CM did not affect the expression of these genes, apart from a significant reduction of *Hes5* expression and a slight increase of *Id1* expression (Fig. 1N; data not shown), corroborating the observation that the bEND3-CM-treated neurospheres retain NSC features. The effects of the bEND3-CM on the size of individual neurospheres were not due to an increase in cell death (Fig. 1O-Q). Rather, phospho-histone H3$^+$ proliferating cells were significantly decreased in the bEND3-CM-treated Sox2$^+$ NSCs (Fig. 1R-T). The effect of bEND3-CM on the number of neurospheres is unlikely to be due to increased cell viability, because the number of apoptotic and necrotic cells remained unchanged after the bEND3-CM treatment (Fig. 1U). Combined, these results suggest that EC-derived signals enhance neurosphere-forming potential but suppress NSC growth in culture.

sAPP enhances neurosphere-forming potential but suppresses NSC growth in culture

To identify EC-derived soluble factors, the CM proteins were fractionated by heparin-affinity chromatography. Based on the fractions' effects on the number and size of neurospheres, we focused on the fraction eluted by 300 mM NaCl (Fig. S2A). Liquid chromatography-mass spectrometry (LC-MS) analysis of the fraction revealed 29 proteins, some of which were examined for their effects on a neurosphere culture derived from acutely dissociated SVZ cells (Fig. S2B,C). Of these, we focused on sAPP because it was also identified from our secreted molecule profiling of the adult SVZ ECs (Lee et al., 2012). Of note, blocking antibodies against sAPP did not affect the number or the size of neurospheres in the bEND3-CM-containing culture, suggesting that other factor(s) may cooperate with sAPP (Fig. S2D,E).

Among different fragments of sAPP (Caille et al., 2004; Ohsawa et al., 1999; Olsen et al., 2014; Willem et al., 2015), the soluble N-terminal fragment (aa 18-286) and the 770 aa form sAPP(770) negatively regulate NSC growth but do not affect the number of neurospheres in the culture from acutely dissociated SVZ cells (Fig. S3). We further evaluated the effect of sAPP(770) on NSC behaviors in the established neurosphere culture (passaged neurospheres). As seen in the bEND3-CM treatment, sAPP(770) increased the number and decreased the size of both primary (Fig. 2A-D) and secondary (Fig. 2E,F) neurospheres while retaining their multipotency (Fig. 2G-L). These data suggest that sAPP(770) enhances neurosphere-forming potential but suppresses NSC growth in culture. sAPP(770) did not affect the expression of the key transcription factors, except for a significant reduction of *Hes5* expression (Fig. 2M; data not shown). sAPP(770) treatment decreased the number of proliferating cells but did not appear to affect cell death in Sox2$^+$ NSCs (Fig. 2N-S). The number of apoptotic and necrotic cells remained unchanged after sAPP(770) treatment (Fig. 2T). These results are similar to the effects of bEND3-CM on NSCs in culture.

APP negatively regulates the SVZ-NSC number *in vivo* in a non-cell-autonomous manner

Previous studies showed that APP is expressed in the SVZ (Caille et al., 2004). To confirm APP expression by an independent method, we performed RT-PCR experiments on acutely isolated ECs from mouse SVZ and cortex by fluorescence-activated cell sorting (FACS). We detected *App* variants in both SVZ and cortex ECs (Fig. S4), indicating that the SVZ ECs express APP, but its expression is not specific to SVZ ECs.

To investigate whether APP plays a similar role in regulating the NSC number *in vivo*, we performed a label-retention assay using 5-bromodeoxyuridine (BrdU) in the adult SVZ of *App* null mutants (Zheng et al., 1995) and their control littermates. BrdU$^+$ label-retaining cells are defined as SVZ-NSCs because the cells have a relatively long cell-cycle time, co-express Sox2 (Fig. S5A,B) and GFAP (data not shown), but do not express any differentiation markers including S100 (Fig. S5C,D). Consistent with previous studies (Shen et al., 2008; Tavazoie et al., 2008), BrdU$^+$ label-retaining NSCs were localized in close proximity to PECAM1$^+$ capillaries in the SVZ (Fig. 3A). *App* null mutants exhibited a

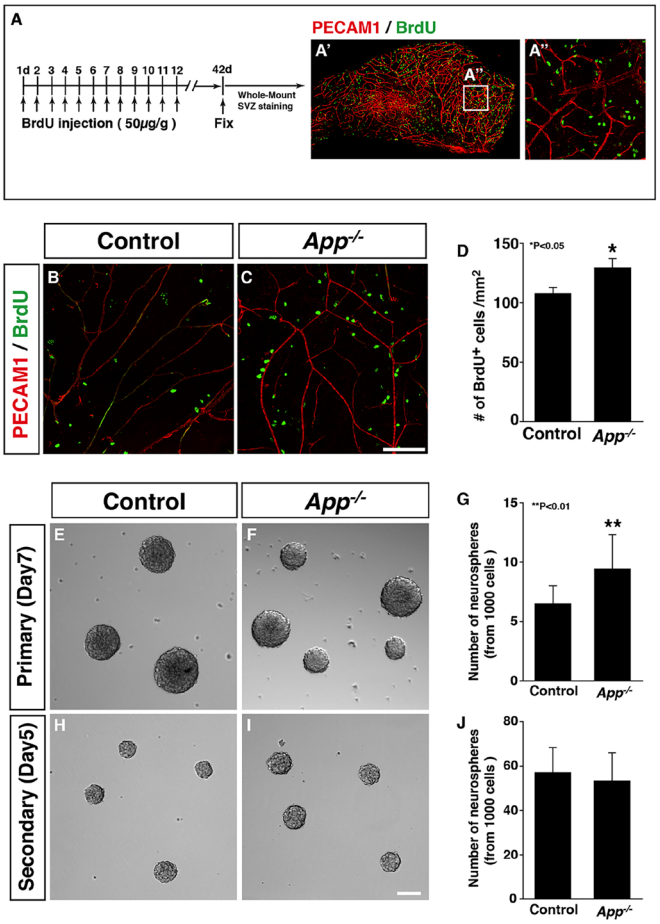

Fig. 3. APP negatively regulates SVZ-NSC number in a non-cell-autonomous manner. (A-A″) Experimental design for a label-retention assay using BrdU in the adult SVZ (A) and whole-mount staining of SVZ with antibodies to the pan-endothelial marker PECAM1 (red) and BrdU indicating label-retaining NSCs (green) (A′,A″). (B,C) Whole-mount staining of *App* mutants and their control littermates with antibodies to PECAM1 (red) and BrdU (green). (D) Quantification of BrdU$^+$ label-retaining NSCs per mm^2. *P<0.05 (Student's t-test). n=18, control SVZ tissues; n=14, mutant SVZ tissues from 7-9 animals. Bars represent mean±s.e.m. (E,F) Images of typical primary neurospheres from acutely dissociated control or *App* mutant SVZ. (G) Quantification of primary neurosphere number. n=14, control; n=15, *App* null mutants from three independent experiments. Bars represent mean±s.d. **P<0.01 (Student's t-test). (H,I) Images of typical secondary neurospheres derived from control or *App* null SVZ-derived primary neurospheres. (J) Quantification of the secondary neurosphere number. n=15, control; n=15, *App* null mutants from three independent experiments. Bars represent mean±s.d. Scale bars:100 µm.

Development (2017) 144, 2730-2736 doi:10.1242/dev.143370

significant increase in the number of BrdU$^+$ label-retaining NSCs in the SVZ, compared with control littermates (Fig. 3B-D). In support of this observation, the mutants yielded more primary neurospheres than did control littermates (Fig. 3E-G). However, there was no significant difference in the number of secondary neurospheres on subcloning (Fig. 3H-J), suggesting that APP negatively regulates NSC number in a non-cell-autonomous manner.

Endothelial APP functions as a negative regulator to control SVZ-NSC number *in vivo*

To address directly whether EC-derived APP controls NSC number *in vivo*, we bred *App*$^{flox/flox}$ mice (Callahan et al., 2017) with an EC-specific *Cre* driver, *Tie2-Cre* (Kisanuki et al., 2001), and an NSC/astrocyte-specific *Cre* driver, *GFAP-Cre* (Zhuo et al., 2001), producing *App*$^{flox/flox}$*;Tie2-Cre* mice and *App*$^{flox/flox}$*;GFAP-Cre* mice, respectively. As seen in the conventional *App* null mutants, more BrdU$^+$ label-retaining NSCs were detected in the SVZ of *App*$^{flox/flox}$*;Tie2-Cre* mice (Fig. 4A-C). In contrast, no change in NSC number was seen in the SVZ of *App*$^{flox/flox}$*;GFAP-Cre* mice (Fig. 4D-F). These data clearly indicate an important role for endothelial APP in determining NSC number in the SVZ.

APP deficiency does not detectably influence SVZ architecture and neuronal differentiation

No significant change in the pinwheel-like arrangement of GFAP$^+$ NSCs, β-catenin$^+$ ependymal cells (Fig. S6A,B) or the SVZ microvascular network (Fig. S6C-E) was observed in *App* mutants. Moreover, the mutants showed no significant change in the amount of doublecortin (DCX)$^+$ neuroblasts (Fig. S6F-H) and Mash1 (Ascl1)$^+$/Ki67 (Mki67)$^+$ transit-amplifying cells in the SVZ (Fig. S6I-K). Likewise, no significant change in the amount of NeuN (Rbfox3)$^+$ post-mitotic neurons in the olfactory bulb was observed (Fig. S6L-O). One possible explanation is that the ∼20% increase in the number of SVZ-NSCs might be overridden by the subsequent expansion of SVZ neural progenitors and the migration of SVZ neuroblasts to the olfactory bulb. These relatively subtle but significant phenotypes in conventional and *App* mutants could indicate that other APP family members may compensate for the loss of APP. Previous studies in mice suggest functional redundancy between APP and APP-like protein 2 (APLP2): APLP2 can take over APP functions *in vivo* (van der Kant and Goldstein, 2015). Indeed, APLP2 was found in the 29 proteins from the bEND3 derived-CM fraction (Fig. S2B) and was also identified from our secreted molecule profiling of the adult SVZ ECs (Lee et al., 2012). It would be interesting to study the functional redundancy between APP and APLP2 by analysis of *App*$^{-/-}$*;Aplp2*$^{-/-}$ double knockout mice.

Conclusions

We present here a normal cell biological role of APP as a negative regulator of NSC growth to control NSC number in the adult SVZ. Given that the major source of SVZ-neurosphere-forming cells are actively dividing *in vivo* and include EGF-responsive activated NSCs but not BrdU$^+$ label-retaining quiescent NSCs (Codega et al., 2014), the observations that sAPP treatment increases the number of neurospheres in culture (our studies) and neurosphere-forming cells *in vivo* (Caille et al., 2004) can be explained by the positive effect of sAPP on the neurosphere-forming potential of activated NSCs. By contrast, sAPP negatively regulates the growth of quiescent NSCs *in vivo* (our studies). These results raise one intriguing question: if sAPP treatment enhances the neurosphere-forming potential in activated NSCs, why does *App* deficiency lead to an increase in the number of neurosphere-forming cells in the SVZ? One possible explanation is that sAPP may be sufficient, but not necessary, to enhance the neurosphere-forming potential *in vivo*: in the *App* mutants, an increase in the number of quiescent NSCs may lead to an increase in the number of neurosphere-forming activated NSCs.

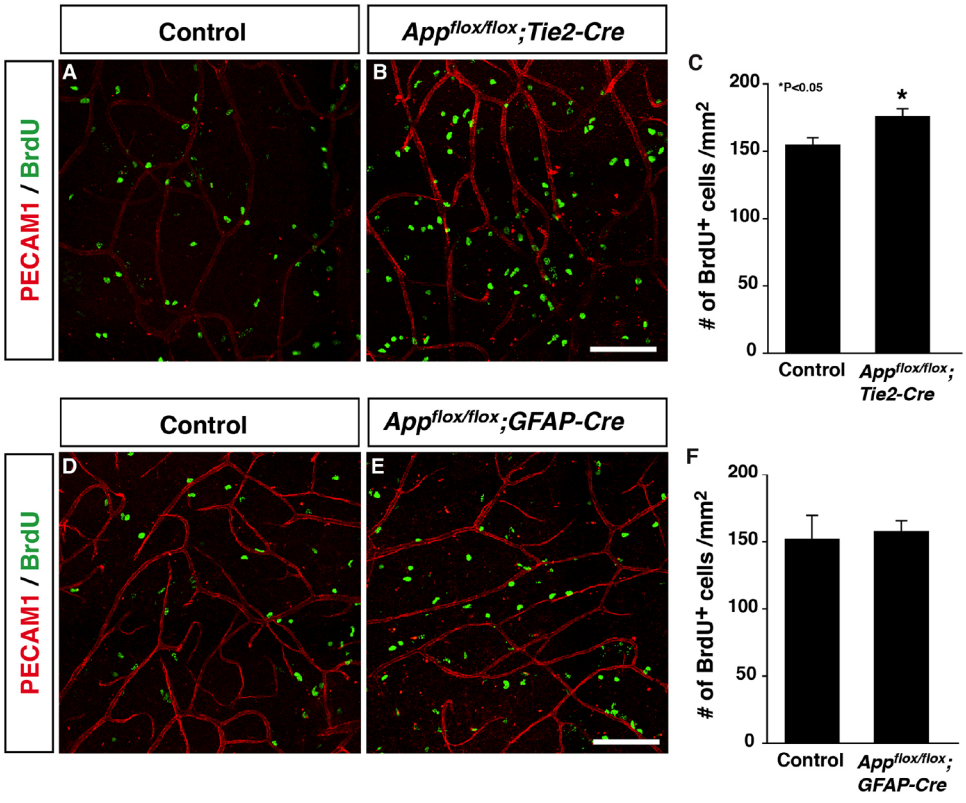

Fig. 4. Endothelial APP is responsible for SVZ-NSC number. (A-C) Whole-mount staining of *App*$^{flox/flox}$*;Tie2-Cre* mutants and their control littermates with antibodies to PECAM1 (red) and BrdU (green) (A,B) and quantification of BrdU$^+$ label-retaining NSCs per mm^2 (C). *P<0.05 (Student's t-test). n=12, control SVZ tissues; n=10, *App*$^{flox/flox}$*;Tie2-Cre* mutant SVZ tissues from 5-6 animals. Bars represent mean±s.e.m. (D-F) Whole-mount staining of *App*$^{flox/flox}$*;GFAP-Cre* mutants and their control littermates with antibodies to PECAM1 (red) and BrdU (green) (D,E) and quantification of BrdU$^+$ label-retaining NSCs per mm^2 (F). n=12, control; n=12, *App*$^{flox/flox}$*;GFAP-Cre* mutants from 6 animals. Bars represent mean±s.e.m. Scale bars:100 µm.

Development (2017) 144, 2730-2736 doi:10.1242/dev.143370

Identification of NSC receptors for sAPP will provide a clearer understanding of the mechanisms by which sAPP regulates the cellular processes of quiescent and activated NSC behaviors.

MATERIALS AND METHODS

Animals

C57BL/6 mice (The Jackson Laboratory), *App* mutants (Zheng et al., 1995) (The Jackson Laboratory), $App^{flox/flox}$ mutants (Callahan et al., 2017), *Tie2-Cre* mice (Kisanuki et al., 2001), *GFAP-Cre* mice (Zhuo et al., 2001) (The Jackson Laboratory), and *Flk1-GFP BAC Tg* mice (Ishitobi et al., 2010) have been reported elsewhere. All experiments were carried out according to the guidelines approved by the National Heart, Lung, and Blood Institute Animal Care and Use Committee.

Preparation of CM from bEND3 cells

bEND3 cells (ATCC) were cultured in the ATCC formulated Dulbecco's Modified Eagle's Medium (DMEM, Gibco/Thermo Fisher Scientific) containing 10% fetal bovine serum (Hyclone Laboratories) and Penicillin-Streptomycin (Gibco/Thermo Fisher Scientific). Preparation of bEND3-derived CM is provided in supplementary Materials and Methods.

Recombinant proteins

The secreted forms of control alkaline phosphatase (AP) and APP were prepared for the neurosphere assay. For details, see supplementary Materials and Methods.

Heparin-agarose fractionation

A total of 500 ml of bEND3 CM was applied to Heparin-Agarose (5 ml bed volume, Sigma). After washing of the column by PBS, the bound proteins were eluted by 30 ml of different concentration of NaCl solution (from 200 mM to 500 mM, every 50 mM). The eluted proteins were concentrated with buffer exchange to PBS through the centrifugal filter unit (Amicon ultra 10K MWCO, Millipore). Each fraction was tested in the neurosphere assay.

Neurosphere culture

Neurospheres were established and cultured as described previously (Ferron et al., 2007) with slight modifications. For details, see supplementary Materials and Methods.

Cell viability assay

Viability of NSCs was assessed as described previously (Ferron et al., 2007). For details, see supplementary Materials and Methods and Table S1.

BrdU labeling and immunohistochemistry

BrdU labeling and whole-mount SVZ immunohistochemistry were performed essentially as described previously (Shen et al., 2008; Tavazoie et al., 2008). All confocal microscopy analysis was carried out on a Leica TCS SP5 confocal (Leica). For details and antibody information, see supplementary Materials and Methods and Table S1.

Flow cytometry

To isolate SVZ and cortex endothelial cells, we used *Flk1-GFP* endothelial cell reporter mice (Ishitobi et al., 2010). All sorting was performed with a FACS Aria (Becton Dickinson). For details, see supplementary Materials and Methods.

RT-PCR

Total RNA was isolated using TRIzol reagent (Ambion) or the RNeasy Mini Kit (QIAGEN) according to the manufacturer's instructions, and reverse-transcribed using SuperScript III (Invitrogen) for PCR. For details and primer information, see supplementary Materials and Methods.

Statistical analysis

Quantification data are represented as means±s.d., means±s.e.m. or box-and-whisker plots. *P*-values were calculated by Student's *t*-test, with $P<0.05$ considered significant. For comparisons across more than two groups, data were analyzed using one-way analysis of variance (ANOVA) with Tukey-HSD multiple comparison test or two-way ANOVA with Sidak correction for multiple comparisons.

Acknowledgements

We thank Y. Chen and M. Gucek for LC-MS assistance; J. Hawkins and the staff of NIH Bldg50 and Bldg14F animal facility for assistance with mouse breeding and care; P. J. McCoy and the staff of the Flow Cytometry Core for FACS assistance; K. Gill for laboratory management and technical support; and R. Reed and F. Baldrey for administrative assistance. Thanks also to R. Adelstein for editorial help and discussion; W. Li for technical help; and S. Kim, B.-N. Koo, J. Msefya, L. Henderson and other members of the Laboratory of Stem Cell and Neuro-Vascular Biology for valuable help and discussion.

Competing interests

The authors declare no competing or financial interests.

Author contributions

Conceptualization: Y.M.; Methodology: Y.S., Y.U., J.H.; Validation: Y.S., Y.U.; Formal analysis: Y.S., Y.U.; Investigation: Y.S., Y.U.; Resources: T.L.Y.-P., T.N.; Writing - original draft: Y.U., Y.M.; Writing - review & editing: Y.S., Y.U., Y.M.; Supervision: Y.M.; Project administration: Y.M.; Funding acquisition: Y.M.

Funding

This work was supported by the Intramural Research Program of the National Heart, Lung, and Blood Institute, National Institutes of Health (HL006115-06 to Y.M.). Deposited in PMC for release after 12 months.

Supplementary information

Supplementary information available online at
http://dev.biologists.org/lookup/doi/10.1242/dev.143370.supplemental

References

Baratchi, S., Evans, J., Tate, W. P., Abraham, W. C. and Connor, B. (2012). Secreted amyloid precursor proteins promote proliferation and glial differentiation of adult hippocampal neural progenitor cells. *Hippocampus* **22**, 1517-1527.

Caille, I., Allinquant, B., Dupont, E., Bouillot, C., Langer, A., Muller, U. and Prochiantz, A. (2004). Soluble form of amyloid precursor protein regulates proliferation of progenitors in the adult subventricular zone. *Development* **131**, 2173-2181.

Callahan, D. G., Taylor, W. M., Tilearcio, M., Cavanaugh, T., Selkoe, D. J. and Young-Pearse, T. L. (2017). Embryonic mosaic deletion of APP results in displaced Reelin-expressing cells in the cerebral cortex. *Dev. Biol.* **424**, 138-146.

Codega, P., Silva-Vargas, V., Paul, A., Maldonado-Soto, A. R., Deleo, A. M., Pastrana, E. and Doetsch, F. (2014). Prospective identification and purification of quiescent adult neural stem cells from their in vivo niche. *Neuron* **82**, 545-559.

Crouch, E. E., Liu, C., Silva-Vargas, V. and Doetsch, F. (2015). Regional and stage-specific effects of prospectively purified vascular cells on the adult V-SVZ neural stem cell lineage. *J. Neurosci.* **35**, 4528-4539.

Delgado, A. C., Ferron, S. R., Vicente, D., Porlan, E., Perez-Villalba, A., Trujillo, C. M., D'Ocon, P. and Farinas, I. (2014). Endothelial NT-3 delivered by vasculature and CSF promotes quiescence of subependymal neural stem cells through nitric oxide induction. *Neuron* **83**, 572-585.

Ferron, S. R., Andreu-Agullo, C., Mira, H., Sanchez, P., Marques-Torrejon, M. A. and Farinas, I. (2007). A combined ex/in vivo assay to detect effects of exogenously added factors in neural stem cells. *Nat. Protoc.* **2**, 849-859.

Gomez-Gaviro, M. V., Scott, C. E., Sesay, A. K., Matheu, A., Booth, S., Galichet, C. and Lovell-Badge, R. (2012). Betacellulin promotes cell proliferation in the neural stem cell niche and stimulates neurogenesis. *Proc. Natl. Acad. Sci. USA* **109**, 1317-1322.

Guo, Q., Li, H., Gaddam, S. S. K., Justice, N. J., Robertson, C. S. and Zheng, H. (2012). Amyloid precursor protein revisited: neuron-specific expression and highly stable nature of soluble derivatives. *J. Biol. Chem.* **287**, 2437-2445.

Ishitobi, H., Matsumoto, K., Azami, T., Itoh, F., Itoh, S., Takahashi, S. and Ema, M. (2010). Flk1-GFP BAC Tg mice: an animal model for the study of blood vessel development. *Exp. Anim.* **59**, 615-622.

Jung, S., Park, R.-H., Kim, S., Jeon, Y.-J., Ham, D.-S., Jung, M.-Y., Kim, S.-S., Lee, Y.-D., Park, C.-H. and Suh-Kim, H. (2010). Id proteins facilitate self-renewal and proliferation of neural stem cells. *Stem Cells Dev.* **19**, 831-841.

Kisanuki, Y. Y., Hammer, R. E., Miyazaki, J.-I., Williams, S. C., Richardson, J. A. and Yanagisawa, M. (2001). Tie2-Cre transgenic mice: a new model for endothelial cell-lineage analysis in vivo. *Dev. Biol.* **230**, 230-242.

Kriegstein, A. and Alvarez-Buylla, A. (2009). The glial nature of embryonic and adult neural stem cells. *Annu. Rev. Neurosci.* **32**, 149-184.

Lee, C., Hu, J., Ralls, S., Kitamura, T., Loh, Y. P., Yang, Y., Mukouyama, Y.-S. and Ahn, S. (2012). The molecular profiles of neural stem cell niche in the adult subventricular zone. *PLoS ONE* **7**, e50501.

Leventhal, C., Rafii, S., Rafii, D., Shahar, A. and Goldman, S. A. (1999). Endothelial trophic support of neuronal production and recruitment from the adult mammalian subependyma. *Mol. Cell. Neurosci.* **13**, 450-464.

Ma, Q.-H., Futagawa, T., Yang, W.-L., Jiang, X.-D., Zeng, L., Takeda, Y., Xu, R.-X., Bagnard, D., Schachner, M., Furley, A. J. et al. (2008). A TAG1-APP signalling pathway through Fe65 negatively modulates neurogenesis. *Nat. Cell Biol.* **10**, 283-294.

Ming, G.-L. and Song, H. (2005). Adult neurogenesis in the mammalian central nervous system. *Annu. Rev. Neurosci.* **28**, 223-250.

Nam, H.-S. and Benezra, R. (2009). High levels of Id1 expression define B1 type adult neural stem cells. *Cell Stem Cell* **5**, 515-526.

Ohsawa, I., Takamura, C., Morimoto, T., Ishiguro, M. and Kohsaka, S. (1999). Amino-terminal region of secreted form of amyloid precursor protein stimulates proliferation of neural stem cells. *Eur. J. Neurosci.* **11**, 1907-1913.

Olsen, O., Kallop, D. Y., McLaughlin, T., Huntwork-Rodriguez, S., Wu, Z., Duggan, C. D., Simon, D. J., Lu, Y., Easley-Neal, C., Takeda, K. et al. (2014). Genetic analysis reveals that amyloid precursor protein and death receptor 6 function in the same pathway to control axonal pruning independent of beta-secretase. *J. Neurosci.* **34**, 6438-6447.

Ottone, C., Krusche, B., Whitby, A., Clements, M., Quadrato, G., Pitulescu, M. E., Adams, R. H. and Parrinello, S. (2014). Direct cell-cell contact with the vascular niche maintains quiescent neural stem cells. *Nat. Cell Biol.* **16**, 1045-1056.

Palmer, T. D., Willhoite, A. R. and Gage, F. H. (2000). Vascular niche for adult hippocampal neurogenesis. *J. Comp. Neurol.* **425**, 479-494.

Rafii, S., Butler, J. M. and Ding, B.-S. (2016). Angiocrine functions of organ-specific endothelial cells. *Nature* **529**, 316-325.

Ramirez-Castillejo, C., Sanchez-Sanchez, F., Andreu-Agullo, C., Ferron, S. R., Aroca-Aguilar, J. D., Sanchez, P., Mira, H., Escribano, J. and Farinas, I. (2006). Pigment epithelium-derived factor is a niche signal for neural stem cell renewal. *Nat. Neurosci.* **9**, 331-339.

Shen, Q., Goderie, S. K., Jin, L., Karanth, N., Sun, Y., Abramova, N., Vincent, P., Pumiglia, K. and Temple, S. (2004). Endothelial cells stimulate self-renewal and expand neurogenesis of neural stem cells. *Science* **304**, 1338-1340.

Shen, Q., Wang, Y., Kokovay, E., Lin, G., Chuang, S.-M., Goderie, S. K., Roysam, B. and Temple, S. (2008). Adult SVZ stem cells lie in a vascular niche: a quantitative analysis of niche cell-cell interactions. *Cell Stem Cell* **3**, 289-300.

Tavazoie, M., Van der Veken, L., Silva-Vargas, V., Louissaint, M., Colonna, L., Zaidi, B., Garcia-Verdugo, J. M. and Doetsch, F. (2008). A specialized vascular niche for adult neural stem cells. *Cell Stem Cell* **3**, 279-288.

van der Kant, R. and Goldstein, L. S. (2015). Cellular functions of the amyloid precursor protein from development to dementia. *Dev. Cell* **32**, 502-515.

Wang, B., Wang, Z., Sun, L., Yang, L., Li, H., Cole, A. L., Rodriguez-Rivera, J., Lu, H.-C. and Zheng, H. (2014). The amyloid precursor protein controls adult hippocampal neurogenesis through GABAergic interneurons. *J. Neurosci.* **34**, 13314-13325.

Wang, S., Bolos, M., Clark, R., Cullen, C. L., Southam, K. A., Foa, L., Dickson, T. C. and Young, K. M. (2016). Amyloid beta precursor protein regulates neuron survival and maturation in the adult mouse brain. *Mol. Cell. Neurosci.* **77**, 21-33.

Willem, M., Tahirovic, S., Busche, M. A., Ovsepian, S. V., Chafai, M., Kootar, S., Hornburg, D., Evans, L. D., Moore, S., Daria, A. et al. (2015). eta-Secretase processing of APP inhibits neuronal activity in the hippocampus. *Nature* **526**, 443-447.

Zhao, C., Deng, W. and Gage, F. H. (2008). Mechanisms and functional implications of adult neurogenesis. *Cell* **132**, 645-660.

Zheng, H., Jiang, M., Trumbauer, M. E., Sirinathsinghji, D. J. S., Hopkins, R., Smith, D. W., Heavens, R. P., Dawson, G. R., Boyce, S., Conner, M. W. et al. (1995). beta-Amyloid precursor protein-deficient mice show reactive gliosis and decreased locomotor activity. *Cell* **81**, 525-531.

Zhuo, L., Theis, M., Alvarez-Maya, I., Brenner, M., Willecke, K. and Messing, A. (2001). hGFAP-cre transgenic mice for manipulation of glial and neuronal function in vivo. *Genesis* **31**, 85-94.